Synthesis, X-ray structure, in vitro HIV and kinesin Eg5 inhibition activities of new arene ruthenium complexes of pyrimidine analogs

Wasfi A. Al-Masoudi, Najim A. Al-Masoudi, Bernhard Weibert & Rainer Winter

View supplementary material ⊞

Accepted author version posted online: 23 May 2017.
Published online: 31 May 2017.

Submit your article to this journal ⊞

Article views: 12

View related articles ⊞

View Crossmark data ⊞

Taylor & Francis
Taylor & Francis Group

Check for updates

Synthesis, X-ray structure, *in vitro* HIV and kinesin Eg5 inhibition activities of new arene ruthenium complexes of pyrimidine analogs

Wasfi A. Al-Masoudi[a], Najim A. Al-Masoudi[b], Bernhard Weibert[c] and Rainer Winter[c]

[a]Department of Physiology, Pharmacology and Chemistry, College of Veterinary, University of Basrah, Basrah, Iraq; [b]Department of Chemistry, College of Science, University of Basrah, Basrah, Iraq; [c]Department of Chemistry, University of Konstanz, Konstanz, Germany

ABSTRACT

Three new ruthenium(II)-arene complexes of the general formula [{(η^6-*p*-cymene)Ru(L)}$_2$](Cl)$_2$), where L are monastrol (**L^1**), ethyl 4-(3-hydroxyphenyl)-6-methyl-2-thioxo-pyrimidine-5-carboxylate (**L^2**) or its 4-bromophenyl analog (**L^3**), have been synthesized and characterized by elemental analysis, ^{1}H, ^{13}C, and 2-D NMR spectroscopy. The X-ray diffraction study of complex **1** showed the presence of a dicationic diruthenium complex where two thioxopyrimidines act as tridentate *μ,κN:κ^{2}S* ligand, bridging two Ru ions through the pyrimidine nitrogen and sulfur atoms. All new complexes were evaluated *in vitro* for their antiviral activity against the replication of HIV-1 and HIV-2 in MT-4 cells using MTT assay. Additionally, complexes **1**–**3** were screened for their inhibitory activity against the ATPase enzyme and the motor-protein Kinesin Eg5. Complex **1** was found to inhibit microtubule-stimulated ATPase activity of kinesin of IC$_{50}$ = 30 μM (monastrol, IC$_{50}$ = 10 μM).
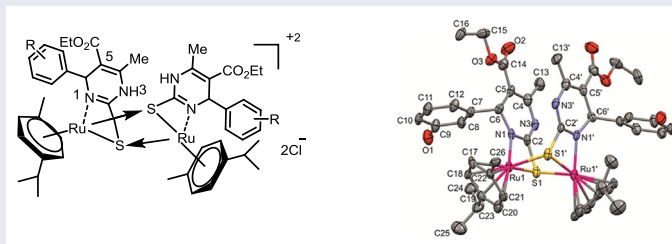
1. Introduction

In recent years, ruthenium-based complexes have emerged as promising antitumor and antimetastatic agents with potential uses in platinum-resistant tumors [1, 2]. Clarke *et al.* reported [Ru(NH$_3$)$_5$(purine)]$^{3+}$ complexes capable of inhibiting DNA and protein synthesis

in human nasopharyngeal carcinoma cells *in vitro* [3] and subsequently initiated interest in ruthenium complexes as potential anticancer pharmaceuticals [4]. Mestroni *et al.* [5] developed six-coordinate Ru(II) complexes with dimethylsulfoxide and chloride ligands with anticancer activity. In 1992, Tocher *et al.* [6] observed the cytotoxicity and anticancer activity of $[(\eta^6\text{-}C_6H_6)RuCl_2(\text{metronidazole})]$. Following this initial study, Dyson and Sadler [7, 8] have focused on the antitumor and antimetastatic activity of arene ruthenium complexes such as $(\eta^6\text{-}p\text{-MeC}_6H_4Pr^i)Ru(P\text{-pta})](Cl_2)$ (pta = 1,3,5-triaza-7-phospha-tricyclo-[3.3.1.1]decane), termed RAPTA-C (Figure 1(A)) [9], and $[(\eta^6\text{-}C_6H_5Ph)Ru(\kappa^2\,N,N\text{-en})Cl]^+\,PF_6^-$ (en = 1,2-ethylenediamine) (Figure 1(B)) and related analogs [10]. Meanwhile, several laboratories have reported the synthesis and anticancer activities of various kinds of organoruthenium complexes. This field has been reviewed competently by Süss-Fink [11, 12]. Currently, two ruthenium compounds, NAMI-A [13, 14] (Figure 1(C)) and KP1019 [9, 15, 16] (Figure 1(D)), which were developed by Sava's and Keppler's work have displayed favorable solubilities and anticancer and antitumor activities in clinical trials [17]. Although RAPTA-C exhibits only a low activity *in vitro*, it is very active *in vivo*, where it inhibits lung metastases in CBA mice. Like NAMI-A, RAPTA-C is also an antimetastatic agent [7] and remains the best anticancer organometallic compound of this series. Recently, Meggers *et al.* [18] developed ruthenium anticancer drugs designed to act as an analog of staurosporine, an effective organic drug protein kinase inhibitor rather than cancer chelation therapy. Even more recently, Li and coworkers have reported that some dinuclear half-sandwich ruthenium complexes with thiosemicarbazone ligands possess higher cytotoxicities against CNE-2, KB, and SGC-7901 cell lines than cisplatin and oxaliplatin [19].

New mitotic targets such as kinesins have also attracted great interest worldwide as potential candidates for a new generation of antiproliferative drugs [20, 21]. Most prominent of these is the kinesin spindle protein (KSP), also known as Eg5, essential for the formation and separation of bipolar spindles during human cell division [22]. The pyrimidine derivative monastrol has been reported to be a specific KSP inhibitor under *in vivo* conditions that inhibits spindle bipolarity and impairs centrosome separation [23].

Given the antitumor and antimetastatic properties of several arene half-sandwich ruthenium complexes and the bioactivity of monastrol, we hoped that combining these two ingredients would create complexes with favorable potency for biomedical applications. In this work, we describe the preparation, characterization, and *in vitro* anti-HIV and kinesin Eg5 inhibitory activity of ruthenium(II) complexes of some pyrimidines related to monastrol.
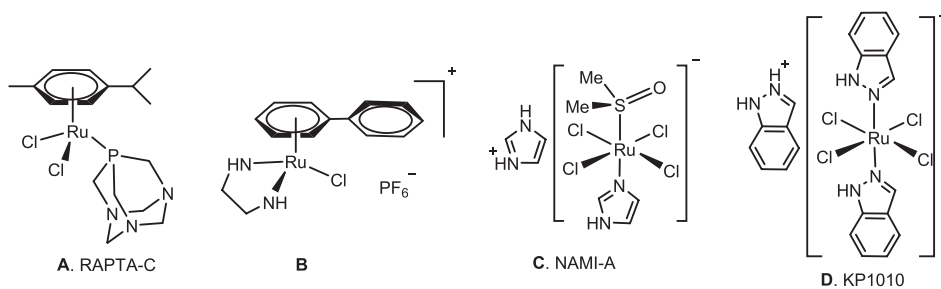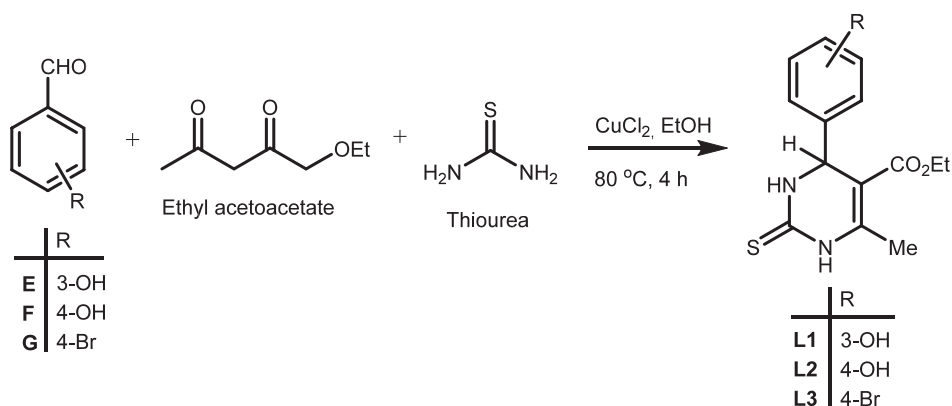

A. RAPTA-C   **B**   **C**. NAMI-A   **D**. KP1010

Figure 1. Some promising anticancer (organo)ruthenium complexes.

Scheme 1. Synthesis of ethyl 4-aryl-6-methyl-2-thioxo-pyrimidine-5-carboxylates (L¹–L³).

2. Experimental

2.1. General procedures and physical measurements

Melting points are uncorrected and were measured on a Büchi melting point apparatus B-545 (Büchi Labortechnik AG, Switzerland). Microanalytical data were obtained using a Vario Elemental Analyzer (Shimadzu, Japan). NMR spectra were recorded on a Bruker Avance III DRX 400 or a Bruker Avance DRX 600 spectrometer, with TMS as internal standard and on the δ scale in ppm. Signal assignments for protons were performed by selective proton decoupling or by COSY spectra. Heteronuclear assignments were verified by HSQC and HMBC experiments. TLC plates 60 F254 were purchased from Merck. The chromatograms were visualized under UV 254–366 nm and iodine (solvent: hexane-ethyl acetate 3:2). [(η^6-p-cymene)RuCl$_2$]$_2$ was prepared according to published procedure [24].

2.2. Synthesis of the ligands: general procedure for preparation of ethyl 4-aryl-6-methyl-2-thioxo-pyrimidine-5-carboxylate derivatives (L¹–L³)

To a stirred mixture of thiourea (1.00 mmol), substituted benzaldehydes **E**–**G** (Scheme 1) (1.00 mmol), ethyl acetoacetate (130 mg, 1.00 mmol), and anhydrous cupric chloride (10 mol%) were added. The mixture was heated at 80°C for 4 h under stirring. After the reaction was completed (checked by TLC), a mixture of H$_2$O:EtOH 8:5 (13 mL) was added and the resulting slurry was stirred at 80°C until total dissolution. After being cooled to room temperature, the reaction mixture was poured onto crushed ice (30 g) and stirred for 5–10 min. The separated solid was filtered under suction (water aspirator), washed with ice-cold water (50 mL), and then recrystallized from hot ethanol to afford the pure product.

2.3. Ethyl-4-(3-hydroxyphenyl)-6-methyl-2-thioxo-pyrimidine-5-carboxylate (monastrol) L¹))

From 3-hydroxybenzaldehyde (**E**) (122 mg). Yield: 216 mg (74%); mp 185–186°C (Lit. [23, 25] 184–186°C).

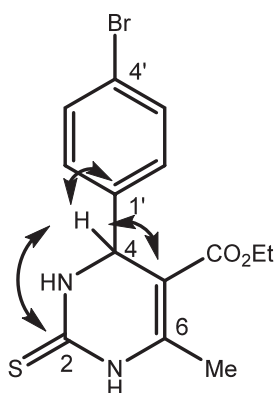For atom numbering refer to Figure 2.

Figure 2. $J_{C,H}$ correlations in the HMBC NMR spectrum of ligand **L³**.

2.4. Ethyl-4-(4-hydroxyphenyl)-6-methyl-2-thioxo-pyrimidine-5-carboxylate (L²) [26]

From 4-hydroxybenzaldehyde (**F**) (122 mg). Yield: 231 mg (79%); mp 203–205°C. ¹H NMR (400 MHz, DMSO-d₆): δ = 10.25 (s, 1H, N*H*), 9.59 (d, 1H, $J_{H3,H4}$ = 5.2 Hz, N*H*), 7.01 (d, 2H, J = 8.6 Hz, H_{arom}), 6.71 (d, 2H, J = 8.6 Hz, $H_{arom.}$), 5.06 (d, 1H, $J_{H3,H4}$ = 5.2 Hz, *H*-4), 4.00 (q, 2H, J = 7.1 Hz, CH_2CH_3), 2.28 (s, 3H, $CH_{3pyrimid}$), 1.10 (t, 3H, J = 7.1 Hz, CH_2CH_3). ¹³C NMR (100 MHz, DMSO-d₆): δ = 14.0 (CH_2CH_3), 17.1 ($C6$-CH_3), 58.5 ($C4_{pyrimid}$), 59.5 (CH_2CH_3), 101.1 ($C5_{pyrimid}$), 115.1 ($C3_{arom+}C5_{arom}$), 127.6 ($C2_{arom}$ + $C6_{arom}$), 134.1 ($C1_{arom}$), 144.5 ($C6_{pyrimid}$), 146.9 ($C4_{arom}$), 165.2 (C=O), 173.7 (C=S). MS (FAB): m/z 292 [M]⁺. Anal. Calcd for $C_{14}H_{16}N_2O_3S\cdot1/2H_2O$ (301.36): C, 55.79; H, 5.35; N, 9.29. Found: C, 55.71; H, 5.66; N, 9.49.

2.5. Ethyl-4-(4-bromophenyl)-6-methyl-2-thioxo-pyrimidine-5-carboxylate (L³)

From 4-bromobenzaldehyde (**G**) (184 mg). Yield: 249 mg (70%); mp 187–190°C. ¹H NMR (400 MHz, CDCl₃): δ = 10.02, 9.27 (2xs, 2H, N*H*), 7.56 (d, 2H, J = 8.2 Hz, $H_{arom.}$), 7.17 (d, 2H, J = 8.2 Hz, $H_{arom.}$), 5.37 (d, 1H, $J_{H3,H4}$ = 5.1 Hz, *H*-4), 4.10 (q, 2H, J = 7.1 Hz, CH_2CH_3), 2.36 (s, 3H, $C6_{pyrimid.}$-CH_3), 1.19 (t, 3H, J = 7.1 Hz, CH_2CH_3). ¹³C NMR (100 MHz, CDCl₃): δ = 14.1 (CH_2CH_3), 18.5 ($C6_{pyrimid.}$-CH_3), 55.7 ($C4_{pyrimid.}$), 60.9 (CH_2CH_3), 102.7 ($C5_{pyrimid.}$), 122.5 ($C4_{arom}$), 128.5 ($C2_{arom}$ + $C6_{arom.}$), 132.1 ($C3_{arom}$ + $C5_{arom}$), 141.3 ($C1_{arom.}$), 142.7 ($C6_{pyrimid}$), 165.0 (C=O), 174.7 (C=S). MS (FAB): m/z 354/356 [M]⁺. Anal. Calcd for $C_{14}H_{15}BrN_2O_2S\cdot H_2O$ (373.25): C, 45.04; H, 4.59; N, 7.50. Found: C, 45.52; H, 4.19; N, 7.68.

2.6. General procedure for synthesis of complexes 1–3

To a stirred solution of pyrimidine derivatives (**L¹**–**L³**) (0.20 mmol) in dry THF (10 mL), solid [(η^6-*p*-cymene)RuCl₂]₂ (**H**) (62 mg, 0.10 mmol) and potassium carbonate (0.20 mmol) were added. The solution was heated under reflux for 6 h under nitrogen. After cooling, the mixture was evaporated to dryness and the residue was washed with diethylether and dried under vacuum to give the desired complex.

The atom numbering for the NMR characterization follows that provided in Scheme 2.
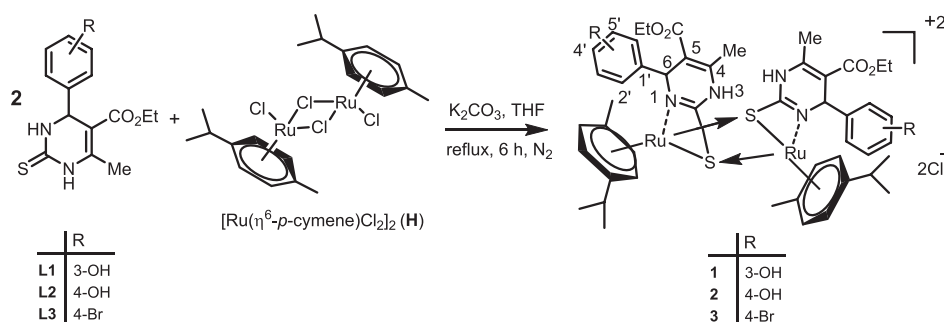
Scheme 2. Synthesis of ruthenium complexes of ethyl 4-aryl-6-methyl-2-thioxo-pyrimidine-5-carboxylate (**1**–**3**).

2.7. Synthesis of [{(η⁶-p-cymene)Ru(L)}₂](Cl)₂) (1)

From **L¹** (59 mg). Yield: 161 mg (68%) as brown crystalline solid; mp 206–209°C. ¹H NMR (600 MHz, CDCl₃): δ = 9.48 (s, 1H, N3H), 7.32 (m, 4H, $H_{arom.}$), 6.29 (m, 4H, $H_{arom.}$), 6.03 (2xd, 8H, J = 7.2 Hz, CH(cymene)), 4.76 (s, 2H, $H6_{pyrimid.}$) 2.99 (sept., 2H, J = 7.4 Hz, CH(CH₃)₂), 2.77 (q, 4H, J = 6.8 Hz, CH_2CH₃), 2.45 (s, 6H, $CH_{3pyrimid.}$), 2.11 (s, 6H, CH_3(cymene)), 1.76 (t, 6H, CH₂CH_3, J = 6.8 Hz), 1.45 (d, 12H, J = 7.4 Hz, CH(CH_3)₂). ¹³C NMR (150.91 MHz, CDCl₃): δ = 14.1 (CH₂CH_3), 17.1 ($CH_{3pyrimid.}$), 17.7 (CH_3(cymene)), 21.5 (CH(CH_3)₂), 29.1 (CH(CH₃)₂), 53.9 (C6$_{pyrimid.}$), 59.5 (CH_2CH₃), 84.6, 86.3, 100.0, 100.8 (6C(cymene)), 113.2 (C3$_{arom.}$), 117.1 (C2$_{arom.}$ + C4$_{arom.}$), 120.4 (C6$_{arom.}$), 121.4 (C5$_{pyrimid.}$), 129.4 (C5$_{arom.}$), 142.8 (C1$_{arom.}$), 144.7 (C2$_{pyrimid.}$), 157.5 (C4$_{pyrimid.}$ + C3$_{arom.}$), 165.2 (C=O). MS (FAB): m/z 1052 ([M−2Cl]⁺). Anal. Calcd for C₄₈H₅₈N₄O₆Ru₂S₂Cl₂·3H₂O (1176.14): C, 49.02; H, 5.31; N, 4.75. Found: C, 49.01; H, 5.53; N, 4.96.

2.8. Synthesis of bis[(η⁶-p-cymene)Ru(L²)]Cl₂ (2)

From **L²** (59 mg). Yield: 89.69 mg (76%) as orange microcrystalline solid; mp 198–201°C. ¹H NMR (600 MHz, CDCl₃): δ = 9.87 (s, 1H, NH), 7.20 (d, 4H, J = 8.0 Hz, H2$_{arom.}$ + H6$_{arom.}$), 6.69 (d, 4H, J = 8.0 Hz, H3$_{arom.}$ + H5$_{arom.}$), 6.01 (d, 4H, J = 6.0 Hz, CH(cymene)), 5.73 (d, 4H, J = 6.0 Hz, CH(cymene)), 4.94 (d, 1H, H2$_{pyrimid.}$), 4.00 (q, 2H, J = 7.0 Hz, CH_2CH₃), 2.82 (sept., 1H, J = 7.3 Hz, CH(CH₃)₂), 2.44 (s, 3H, $CH_{3pyrimid.}$), 2.25 (s, 3H, CH_3(cymene)), 1.22 (d, 6H, CH(CH_3)₂), 1.16 (t, 3H, J = 7.0 Hz, CH₂CH_3). ¹³C NMR (150.91 MHz, CDCl₃): δ = 14.0 (CH₂CH_3), 17.2 ($CH_{3pyrimid.}$), 17.9 (CH_3(cymene)), 21.5 (CH(CH_3)₂), 29.9 (CH(CH₃)₂), 53.7 (C6$_{pyrimid.}$), 59.8 (CH_2CH₃), 85.5, 86.4, 100.2, 100.6 (6C(cymene)), 117.1 (C3$_{arom.}$ + C5$_{arom.}$), 120.5 (C5$_{pyrimid.}$), 129.7 (C2$_{arom.}$ + C6$_{arom.}$), 135.6 (C1$_{arom.}$), 144.5 (C2$_{pyrimid.}$), 157.8 (C4$_{pyrimid.}$ + C4$_{arom.}$), 165.2 (C=O). MS (FAB): m/z 1052 ([M−2Cl]⁺). Anal. Calcd for C₄₈H₅₈N₄O₆Ru₂S₂Cl₂·3H₂O (1176.14): C, 49.02; H, 5.31; N, 4.75. Found: C, 48.88; H, 5.49; N, 4.31.

2.9. Synthesis of bis[(η⁶-p-cymene)Ru(L³)]Cl₂ (3)

From **L³** (71 mg). Yield: 61.10 mg (86%) as brown microcrystalline solid; mp 173–175°C. ¹H NMR (600 MHz, CDCl₃): δ = 9.97 (s, 1H, NH), 7.41 (d, 4H, J = 8.0 Hz, H3$_{arom.}$ + H5$_{arom.}$), 7.12 (d, 4H, J = 8.0 Hz, H2$_{arom.}$ + H6$_{arom.}$), 5.39 (br s., 2H, H6$_{pyrimid.}$), 5.31 (d, 4H, J = 5.3 Hz, CH(arene)), 5.20 (d, 4H, J = 5.3 Hz, CH(cymene)), 3.48 (q, 4H, J = 7.0 Hz, CH_2CH₃), 2.98 (sept., 2H, J = 6.8 Hz,

$CH(CH_3)_2$), 2.35 (s, 6H, $CH_{3pyrimid.}$), 2.24 (s, 6H, CH_3(cymene), 1.31 (d, 12H, $J = 6.8$ Hz, CH($CH_3)_2$), 1.21 (t, 6H, $J = 7.0$ Hz, CH_2CH_3). ^{13}C NMR (150.91 MHz, CDCl$_3$): $\delta = 14.1$ (CH_2CH_3), 18.2 ($CH_{3pyrimid.}$), 18.4 (CH_3(cymene)), 22.6 (CH($CH_3)_2$), 30.5 (CH(CH$_3)_2$), 55.0 ($C6_{pyrimid.}$), 60.7 (CH_2CH_3), 88.7, 89.0, 103.4, 103.5 (6C(cymene)), 122.6 ($C5_{pyrimid.}$), 125.3 ($C4_{arom.}$), 128.8, 129.0 ($C2_{arom.}$, $C6_{arom.}$ and $C3_{arom.}$, $C5_{arom.}$), 140.3 ($C1_{arom.}$), 143.3 ($C2_{pyrimid.}$), 156.5 ($C4_{pyrimid.}$), 164.8 ($C = O$). MS (FAB): m/z 1178/1176 ([M–2Cl]$^+$). Anal. Calcd for $C_{48}H_{54}Br_2N_4O_4Ru_2S_2Cl_2 \cdot 6H_2O$ (1356.04): C, 42.52; H, 4.91; N, 4.13. Found: C, 42.43; H, 4.63; N, 4.32.

2.10. *Crystallographic structure determination*

Complex **1** crystallized as brownish-orange blocks from a CH_2Cl_2/CH_3OH mixture as the methanol disolvate. X-ray diffraction measurements were performed on a STOE IPDS-II diffractometer. The data were processed using the SAINT software [27]. Crystal data, data collection parameters, and structure refinement details are given in Table 1. The structure was solved by direct methods and refined by full-matrix least-squares techniques. Non-hydrogen atoms were refined with anisotropic displacement parameters. Hydrogens were inserted in calculated positions and refined with a riding model. The following computer programs were used: structure solution, SHELXL [28]; molecular diagrams, ORTEP [29].

2.11. **In vitro *anti-Kinesin Eg5 assay***

The ATPase activity of the Eg5 motor domain was measured using the malachite green assay as described earlier [30]. The reactions were performed in reaction buffer (80 mM Pipes, pH

Table 1. Crystal data and details of data collection for **1**.

Empirical formula	$C_{25}H_{32}ClN_2O_4SRu$
Fw	593.10
Wavelength (Å)	0.71073
Crystal system	Orthorhombic
Space group	*Pcan*
Unit cell dimensions	$a = 14.805(3)$ Å, $\alpha = 90°$
	$b = 16.179(2)$ Å, $\beta = 90°$
	$c = 21.834(3)$ Å, $\gamma = 90°$
V (Å)	5229.7(14) Å^3
Z	8
λ (Å)	0.71073
D_{calcd}	1.507 mg m^{-3}
Crystal size	$0.3 \times 0.2 \times 0.1$ mm^3
T (K)	100(2)
θ range for data collection (°)	1.865 to 26.117
μ(MoKα)	0.815 mm^{-1}
$R_1{}^a$	0.0940
$wR_2{}^b$	0.1407
GOF^c	1.104
$\Delta\rho_{fin}$ (max/min)	1.144/−0.782 e Å^{-3}
Independent reflections	5160 [R(int) = 0.2634]
Absorption coefficient	0.815 mm^{-1}
F(0 0 0)	2440
Index ranges	h, k, l- 18/18, ± 19, ± 26
Reflections collected	66,810
Completeness to $\theta = 25.242°$	100.0%

$^a R_1 = \Sigma ||F_o| - |F_c||/\Sigma |F_o|$.
$^b wR_2 = \{\Sigma[w(F^2_o - F^2_c)^2/\Sigma[w(F^2_o)^2]\}^{1/2}$.
^{c}GOF $= \{\Sigma[w(F^2_o - F^2_c)^2] /(n\text{-}p)\}^{1/2}$, where n is the number of reflections and p is the total number of parameters refined.

6.8; 1 mM EGTA, 1 mM $MgCl_2$, 0.1 mg/mL BSA, 1 mM taxol) supplemented with Eg5 (48 nM) fusion protein and microtubules (200 nM). Ten minutes after the addition of the compound, reactions were started by the addition of ATP (50 mM) and incubated at RT for 7 min. The reactions were stopped by adding perchloric acid (444 mM, Fluka), and the color reaction was started by adding the developer solution (1 M HCl (Sigma), 33 mM malachite green (Sigma), 775 mM ammonium molybdatetetrahydrate (Sigma)). After 20 min, the absorbance at 610 nm was measured using a plate reader (Victor 2, Perkin-Elmer). The IC_{50} values were determined in three independent experiments for each compound.

2.12. In vitro *anti-HIV assay*

Evaluation of the antiviral activity of ligands **L¹**–**L³** and compounds **H** and **1**–**3** against the HIV-1 strain (III_B) and the HIV-2 strain (ROD) in MT-4 cells was performed using an MTT assay as described previously [31]. In brief, stock solutions (10-times final concentration) of test compounds were added in 25-μL volumes to two series of triplicate wells to allow simultaneous evaluation of their effects on mock and HIV-infected cells at the beginning of each experiment. Serial five-fold dilutions of test compounds were made directly in flat-bottomed 96-well microtiter trays using a Biomek 3000 robot (Beckman instruments). Untreated control, HIV- and mock-infected cell samples were included for each sample. HIV-1 (III_B) [32] or HIV-2 (ROD) [33] stock (50 μL) at 100–300 CCID50 (50% cell culture infectious dose) or culture medium was added to either of the infected or mock-infected wells of the microtiter tray. Mock-infected cells were used to evaluate the effect of test compound on uninfected cells in order to assess the cytotoxicity of the test compounds. Exponentially growing MT-4 cells [34] were centrifuged for 5 min at 1000 rpm (Minifuge T, rotor 2250; Heraeus, Germany), and the supernatant was discarded. The MT-4 cells were resuspended at 6×10^5 cells per mL, and volumes of 50 μL were transferred to the microtiter tray wells. Five days after infection, the viability of the mock- and HIV-infected cells was examined spectrophotometrically.

3. Results and discussion

3.1. Synthesis of the ligands

In the past decade, ruthenium arene complexes have received considerable attention as anticancer agents and because of their favorable properties such as chemical stability and structural diversity [7–12]. Therefore, our attention was drawn to the synthesis of new ruthenium complexes containing monastrol and closely related conjugated pyrimidine derivatives, aiming to study their potential application as anti-HIV agents or as inhibitors for kinesin Eg5. Thus, ligands **L¹**–**L³** have been prepared in 70–79% yield, via the Biginelli reaction, *i.e.* in a one-pot, three-component cyclocondensation reaction of substituted benzaldehyde **E**–**G**, ethyl acetoacetate and thiourea in the presence of catalytic amounts of $CuCl_2$ (Scheme 1). The literature reports various Lewis acids as catalyst in optimizing the yield of pyrimidines [35].

Ligand **L³** was selected for further NMR studies to aid the signal assignment and its HMBC [36] spectrum revealed a $^2J_{C,H}$ coupling between H4 of the pyrimidine ring at 5.37 ppm and the aromatic carbon atom 1′ at 141.3 ppm. In addition, $^2J_{C,H}$ coupling between H4 and C5 at 102.7 ppm was observed. Furthermore, a $^3J_{C,H}$ coupling between H4 and the C=S carbon atom at 174.7 ppm was detected (Figure 2).

3.2. Synthesis of the complexes

Complexes of the general formula $[\{(\eta^6\text{-}p\text{-cymene})Ru(L)\}_2](Cl)_2)\cdot nH_2O$ (**1**–**3**) (Scheme 2) were prepared by a typical μ-chlorido-bridge splitting reaction of $[Ru(\eta^6\text{-}p\text{-cymene})Cl_2]_2$ (**H**) with the corresponding ligands **L¹**–**L³** in a 1:2 molar ratio in refluxing THF and K_2CO_3 under nitrogen. The complexes precipitated directly from the reaction mixture after concentration of the solutions under reduced pressure and were isolated in yields of 68 to 86%.

The structures of complexes **1**–**3** have been identified by their ¹H, ¹³C, mass and 2D NMR spectra. The ¹H NMR spectra showed the characteristic pattern of the p-cymene moiety with methyl singlets at 2.08–2.25 ppm, doublets at 1.22–1.43 ppm for the CH(CH₃)₂ groups and a septet at 2.82–2.99 ppm for CH(CH₃)₂ as well as the typical set of two doublets for the aryl-CH protons in the range of 6.0 to 5.2 ppm. The resonance of proton H6 at the pyrimidine backbone appeared as a (broad) singlet at 4.77, 4.94 or 5.39 ppm, respectively. The aromatic protons of the complexes resonated as multiplet or doublets at 6.28–7.41 ppm. The ¹³C NMR spectra for complexes **1**–**3** displayed all expected resonances for the carbon atoms of the p-cymene ring. The carbon atoms at position 2 of pyrimidine ring (N = C–S) of complexes **1**–**3** appeared at ca. 144 ppm, and thus at ca. 30 ppm higher-field compared to the thiocarbonyl carbon atom of the corresponding free ligand. This sizable upfield shift is indicative for complexation of the ligands **L¹**–**L³** by the cymene ruthenium half-sandwich fragment via a thiolate function. In addition, C5 of pyrimidine moiety resonated at ca. 121 ppm, whereas the carbon resonance of C4 of the same ring appeared at ca. 157 ppm. The expected resonance signals of the appended phenyl ring and the ester function were also observed and assigned (c.f. Experimental section).

3.3. X-ray crystal structure

The result of the X-ray diffraction study of **1** (as methanol disolvate) is shown in Figure 3 with selected bond distances and angles given in Table 2. The C_2 symmetric diruthenium
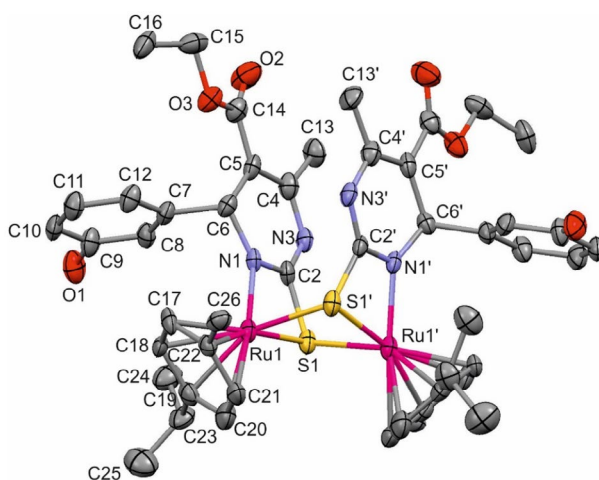

Figure 3. ORTEP view of the molecule of $[(\eta^6\text{-}p\text{-cymene})Ru(L^1)]$ (**1**) in the crystal. Displacement ellipsoids are drawn at 50% probability level.

Table 2. Selected bond lengths [Å] and angles [°] for **1**.

Bond lengths		Bond angles	
Ru1–S1′	2.422(3)	S1–Ru1–S1′	83.07(7)
Ru1–S1	2.423(3)	Ru1–S1–Ru1′	93.25(7)
Ru1–C2	1.766(9)	S1–Ru1–N1	67.08(19)
Ru1–N1	2.102(7)	S1′–Ru–N1	87.92(19)
C2–S1	1.766(9)	S1–C2–N1	110.1(7)
C2–N1	1.282(10)	C2–N1–Ru1	103.8(6)
N3–C4	1.370(12)	N1–C2–N3	125.4(8)
C4–C5	1.381(12)	C2–N1–C6	121.8(7)
C5–C6	1.514(12)	N1–C6–C5	111.4(7)
N1–C6	1.479(10)	C4–C5–C6	120.7(8)
		C2–N3–C4	119.5(7)

complex **1** crystallized in the *Pcan* space group belonging to the orthorhombic crystal system with four identical molecules within the unit cell. The arene ruthenium moieties adopt the archetypical three-legged, piano-stool structure. Bond angles subtended by the ligands forming the legs and the ruthenium atom are all close to 90° (N1–Ru1–S1 = 87.90(19)°, C21–Ru1–S1 = 89.8(3)°, S1–Ru1–S1′ = 83.07(7)° and attest to the overall *pseudo*-octahedral coordination of the metal atom. The 4-aryl-6-methyl-2-thioxopyrimidine-5-carboxylate ligand is present in its unideprotonated, monoanionic form and adopts the iminothiolate tautomeric structure as indicated by the short C(2)–N(1) bond length of 1.284(11) Å and a C–S single bond length C2–S1 of 1.764(10) Å. The latter value is within the range of a C_{ar}–S single bond (1.773(9) Å), while the C(2)–N(1) bond is appreciably shorter than the delocalized intracyclic C_{aryl} = N double bond of pyrimidine heterocycles (1.333(13) Å) [37]. The ligand L acts as a tridentate bridging ligand in the $\mu,\kappa N:\kappa^2 S$ binding mode, coordinating to one Ru atom via the pyrimidine N1 nitrogen atom and bridging two ruthenium atoms via the thiolate donor S1. The central Ru_2S_2 ring is distinctly puckered with a dihedral angle of 30.2° between the Ru_2S flaps. The long Ru···Ru distance of 3.522 Å demonstrates that the present complex belongs to the class of dinuclear ligand-bridged, half-sandwich ruthenium complexes with no direct bonding interactions between the Ru atoms [38]. The central Ru_2S_2 ring is annealed to two kite-shaped, almost planar four-membered rings comprising atoms Ru1, S1, C2 and N1, which are almost planar with an angle sum of 351.7° and an interplanar angle between the S1,Ru1,N1 and the S1,C2,N1 planes of 2.7°. These four-membered rings are in a *cis*-arrangement and are symmetry-related by a twofold rotational axis passing through the midpoint of the Ru_2S_2 ring. This arrangement forces the two four- and the annealed six-membered thiooxopyrimidine rings into a cofacial, slightly tilted arrangement with an interplanar angle of 13.3° and a centroid-to-centroid distance of 3.313 Å. The thiooxopyrimidine rings are notably planar despite the sp³ hybridization of carbon atom C6. The overall structural features and arrangement of the core of the three annealed four-membered rings resembles closely those published very recently for diruthenium thiosemicarbazone complexes [19]. This overall similarity also pertains to the Ru–S and the Ru–N bond lengths of 2.422(3) and 2.423(3) Å or 2.101(7) Å, which all fall in the range of the seven related diruthenium complexes with thiosemicarbazone ligands (range 2.3999(1) to 2.434(4) Å and 2.0371(1) to 2.1287(1) Å). The Ru–C(cymene) bond lengths vary from 2.174(12) Å to 2.233(9) Å. In **1**, the longest Ru–C bond involves the carbon atom C(17) as it is observed for many cymene ruthenium complexes. We note here that other related diruthenium thiosemicarbazone-bridged complexes usually prefer the *N,N* binding mode of the ligand with

Table 3. *In vitro* anti-HIV-1[a] and HIV-2[b] activity of some pyrimidines and their ruthenium(II)-cymene complexes.

Compd.	Virus strain	EC_{50} (µg/mL)[c]	CC_{50} (µg/mL)[d]	SI[e]
L^1	III_B	> 11.24	> 11.24	< 1
	ROD	> 11.24	> 11.24	< 1
L^2	III_B	> 66.50	> 66.50	< 1
	ROD	> 66.50	> 66.50	< 1
L^3	III_B	> 11.68	11.68	< 1
	ROD	> 11.68	11.68	< 1
H	III_B	> 125	> 125.00	X1
	ROD	> 125	> 125.00	X1
1	III_B	> 75.45	75.45	< 1
	ROD	> 75.45	75.45	< 1
2	III_B	> 85.35	85.35	< 1
	ROD	> 85.35	85.35	< 1
3	III_B	> 43.55	> 43.55	< 1
	ROD	> 43.55	> 43.55	< 1
Lamuvidine	III_B	0.58	0.13	> 34
	ROD	2.27	0.13	> 9
Nevirapine	III_B	0.075	> 4	> 80
	ROD	> 4	> 4	X1

[a]Anti-HIV-1 activity measured on strain III_B.
[b]Anti-HIV-2 activity measured using strain ROD.
[c]Compound concentration required to achieve 50% protection of MT-4 cells from HIV-1 to HIV-2 induced cytopathogenic effects.
[d]Compound concentration that reduces the viability of mock-infected MT-4 cells by 50%.
[e]Selectivity index (CC_{50}/EC_{50}).

concomitant formation of five-membered chelate rings and significantly shorter Ru–N bonds of 2.077(5) to 2.093(5) Å [38, 39].

3.4. In vitro *anti-HIV activity*

Compounds L^1–L^3, **H,** and **1**–**3** were evaluated for their *in vitro* anti-HIV-1 (strain III_B) and anti-HIV-2 (strain ROD) activity and monitored by the inhibition of the virus-induced cytopathic effect in the MT-4 cells, based on an MTT assay [31]. The results are summarized in Table 3, in which the data for lamuvidine [40] and nevirapine (BOE/BIRG587) [41] are included for comparison. None of the tested compounds were active against inhibition of HIV-1 and HIV-2. However, the antimitotic agent (monastrol, L^1) and the 3-bromophenyl analog L^3 exhibited EC_{50} values of 11.24 and 11.68 µg/mL, respectively, with no selectivity observed (SI < 1). It is noteworthy to mention that the ligands L^1 and L^3 showed much more HIV inhibitory activity than their ruthenium-cymene complexes **1** and **3** (EC_{50} > 75.45 and > 43.55 µg/mL), respectively, which means that ruthenium coordination has a detrimental effect on their potency to HIV inhibition.

3.5. In vitro *anti-kinesin Eg5 activity*

Kinesin-5 motor proteins act to separate the spindle poles during formation of the bipolar mitotic spindle [42]. Monastrol (MA) has been reported as one of these antimitotic agents that is capable of arresting cells in mitosis by specifically inhibiting Eg5 [25, 43]. Like many enzyme inhibitors, monastrol might be substrate competitive, inhibiting the ATP hydrolysis cycle of Eg5 by directly competing with ATP [42, 44], or by microtubule binding. Alternatively,
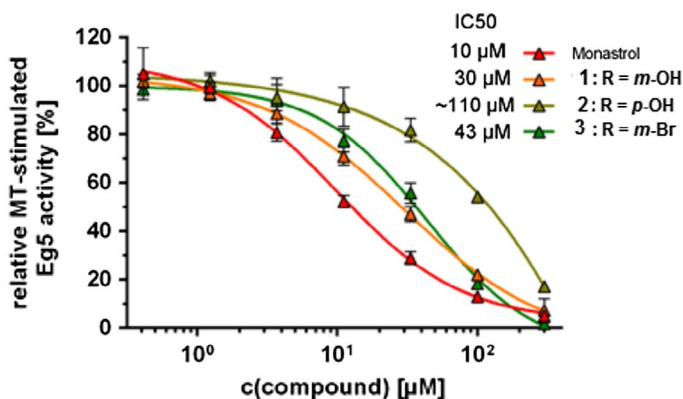
Figure 4. Inhibition concentrations (IC$_{50}$) in µM of monastrol and the new ruthenium complexes **1**–**3** for Eg5-driven microtubule motility.

monastrol might inhibit the motor domain allosterically, either by inhibiting ATP hydrolysis or by uncoupling partner head interactions to inhibit motor, but not ATPase activity [45].

Organometallic ruthenium-arene compounds bearing a maltolate ligand have been shown to be nearly inactive in cytotoxicity assays. However, dinuclear ruthenium-arene derivatives were found to show cytotoxic activity against cancer cells, which increases with the spacer length between the metal centers [46]. For this reason, complexes **1**–**3** have been screened for their inhibition of Eg5 activity using an *in vitro* malachite green ATPase assay (enzyme-coupled assay) [47]. Complex **1** exhibited IC$_{50}$ value of 30 µM and turned out to show the best performance of all complexes of this series. None of the present compounds matches, however, the criteria of a selective inhibitor of Eg5 in this assay in comparison to monastrol (IC$_{50}$ = 10 µM, Figure 4).

4. Conclusion

A series of η^6-*p*-cymene ruthenium complexes with 4-aryl-2-thioxopyrimidine ligands were synthesized and characterized. Spectroscopic data agree with binding of the ligands as unideprotonated N–S chelates. The molecular structure of complex **1** showed a ligand-bridged diruthenium structure with a central Ru$_2$S$_2$ core and two cofacially arranged four-membered Ru,S,C,N rings, which are constructed from two (*p*-cymene)Ru fragments and two bridging tridentate 2-thiooxpyrimidine ligands in a $\mu,\kappa N{:}\kappa^2 S$ binding mode. The *in vitro* anti-HIV-1 and HIV-2 activities of the ligands and the complexes were investigated, and the compounds were found to be inactive. Additionally, the complexes have been screened for their inhibitory activity against protein kinesin Eg5. None of these compounds matched the criteria of a selective inhibitor of Eg5 in this assay in comparison to monastrol (IC$_{50}$ = 10 µM).

Supplementary material

Disclosure statement

No potential conflict of interest was reported by the authors.

References

[1] E.S. Antonaraki, E. Emadi. *Cancer Chemother. Pharmacol.*, **66**, 1 (2010).
[2] N.P. Barry, P.J. Sadler. *Chem. Commun.*, **49**, 5106 (2013).
[3] A.D. Kelman, M.J. Clarke, S.D. Edmonds, H.J. Peresie. *Clin. Hematol. Oncol.*, **7**, 74 (1977).
[4] M.J. Clarke. In *Metal Complexes as Anticancer Agents*, H. Sigel (Ed.), pp. 231–283, CRC Press, USA (1980).
[5] G. Mestroni, E. Alessio, M. Calligaris, W.M. Attia, F. Quadrifoglio, S. Cauci, G. Sava, S. Zorzet, S. Pacor. In *Ruthenium and Other Non-Platinum Metal Complexes in Cancer Chemotherapy*, E. Alessio, M.J. Clarke (Eds.), pp. 71–87, Springer-Verlag, Berlin, New York (1989).
[6] L.D. Dale, J.H. Tocher, T.M. Dyson, D.I. Edwards, D.A. Tocher. *Anticancer Drug Des.*, **7**, 3 (1992).
[7] P.J. Dyson. *Chimia*, **61**, 698 (2007).
[8] S.J. Dougan, P.J. Sadler. *Chimia*, **61**, 704 (2007).
[9] C.S. Allardyce, P.J. Dyson, D.J. Ellis, S.L. Heath. *Chem. Commun.*, 1396–1397 (2001).
[10] R.E. Morris, R.E. Aird, P. del Socorro Murdoch, H.M. Chen, J. Cummings, N.D. Hughes, S. Parsons, A. Parkin, G. Boyd, D.I. Jodrell, P.J. Sadler. *J. Med. Chem.*, **44**, 3616 (2001).
[11] G. Süss-Fink. *Dalton Trans.*, **39**, 1673 (2010).
[12] J. Furrer, G. Süss-Fink. *Coord. Chem. Rev.*, **309**, 36 (2016).
[13] A. Bergamo, G. Sava. *Dalton Trans.*, **13**, 1267 (2007).
[14] G. Sava, A. Bergamo, S. Zorzet, B. Gava, C. Casarsa, M. Cocchietto, A. Furlani, V. Scarcia, B. Serli, E. Iengo, E. Alessio, G. Mestroni. *Eur. J. Cancer*, **38**, 427 (2002).
[15] C.G. Hartinger, S. Zorbas-Seifried, M.A. Jakupec, B. Kynast, H. Zorbas, B.K. Keppler. *J. Inorg. Biochem.*, **100**, 891 (2006).
[16] F. Lentz, A. Drescher, A. Lindauer, M. Henke, R.A. Hilger, C.G. Hartinger, M.E. Scheulen, C. Dittrich, B.K. Keppler, U. Jaehde. *Anticancer Drugs*, **20**, 97 (2009).
[17] C.G. Hartinger, M.A. Jakupec, S. Zorbas-Seifried, M. Groessl, A. Egger, W. Berger, H. Zorbas, P.J. Dyson, B.K. Keppler. *Chem. Biodivers.*, **5**, 2140 (2008).
[18] H. Bregman, P.J. Carroll, E. Meggers. *J. Am. Chem. Soc.*, **128**, 877 (2006).
[19] W. Su, Z. Tang, P. Li, G. Wang, Q. Xiao, Y. Li, S. Huang, Y. Gu, Z. Laid, Y. Zhang. *Dalton Trans.*, **45**, 19329 (2016).
[20] D. Huszar, M.E. Theoclitou, J. Skolnik, R. Herbst. *Cancer Metastasis Rev.*, **28**, 197 (2009).
[21] S.D. Knight, C.A. Parrish. *Curr. Top. Med. Chem.*, **8**, 888 (2008).
[22] C.J. Lawrence, R.K. Dawe, K.R. Christie, D.W. Cleveland, S.C. Dawson, S.A. Endow, L.S. Goldstein, H.V. Goodson, N. Hirokawa, J. Howard, R.L. Malmberg, J.R. McIntosh, H. Miki, T.J. Mitchison, Y. Okada, A.S. Reddy, W.M. Saxton, M. Schliwa, J.M. Scholey, R.D. Vale, C.E. Walczak, L. Wordeman. *J. Cell Biol.*, **167**, 19 (2004).
[23] T.U. Mayer, T.M. Kapoor, S.J. Haggarty, R.W. King, S.L. Schreiber, T.J. Mitchison. *Science*, **286**, 971 (1999).
[24] M.A. Bennett, T.-N. Huang, T.W. Matheson, A.K. Smith, S. Ittel, W. Nickerson. *Inorg. Synth.*, **21**, 74 (1982).
[25] D. Dallinger, C.O. Kappe. *Nat. Protoc.*, **2**, 317 (2007).

[26] B. Liu, M. Zhang, N. Cui, J. Zhu, J. Cui. *Acta Cryst.*, **E64**, 261 (2008).
[27] *SAINT-Plus, Version 7.06a and APEX2*, Bruker-Nonius AXS Inc., Madison, WI (2004).
[28] G.M. Sheldrick. *Acta Crystallogr., Sect. C*, **71**, 3 (2015).
[29] M.N. Burnett, G.K. Johnson. *ORTEPIII. Report ORNL-6895*, OAK Ridge National Laboratory, Tennessee, USA (1996).
[30] D.J. Sharp, G.C. Rogers, J.M. Scholey. *Nature*, **407**, 41 (2000).
[31] C. Pannecouque, D. Daelemans, E. De Clercq. *Nat. Protoc.*, **3**, 427 (2008).
[32] M. Popovic, M.G. Sarngadharan, E. Read, R.C. Gallo. *Science*, **224**, 497 (1984).
[33] F. Barré-Sinoussi, J.C. Chermann, F. Rey, M.T. Nugeyre, S. Chamaret, J. Gruest, C. Alxer-Blin, F. Vézinet-Brun, C. Rouzioux, W. Rozenbaum, L. Montagnier. *Science*, **220**, 868 (1983).
[34] I. Miyoshi, H. Taguchi, I. Kobonishi, S. Yoshimoto, Y. Ohtsuki, Y. Shiraishi, T. Akagi. *Gann. Monogr. Cancer Res.*, **28**, 219 (1982).
[35] N.A. Al-Masoudi, N.J. Al-Salihi, Y.A. Marich, T. Markus. *J. Fluoresc.*, **26**, 31 (2016).
[36] W. Willker, D. Leibfritz, R. Kerssebaum, W. Bermel. *Magn. Reson. Chem.*, **31**, 287 (1993).
[37] D.R. Lide. *CRC Handbook of Chemistry and Physics*, 76th Edn. 9.7 and 9.9 (1995–1996).
[38] B. Demoro, C. Sarniguet, R. Sánchez-Delgado, M. Rossi, D. Liebowitz, F. Caruso, C. Olea-Azar, V. Moreno, A. Medeiros, M.A. Comini, L. Otero, D. Gambino. *Dalton Trans.*, **41**, 1534 (2012).
[39] B. Demoro, M. Rossi, F. Caruso, D. Liebowitz, C. Olea-Azar, U. Kemmerling, J.D. Maya, H. Guiset, V. Moreno, C. Pizzo, G. Mahler, L. Otero, D. Gambino. *Biol. Trace Elem. Res.*, **153**, 371 (2013).
[40] J.A. Coates, N. Cammack, H.J. Jenkinson, A.J. Jowett, B.A. Pearson, C.R. Penn, P.L. Rouse, K.C. Viner, J.M. Cameron. *Antimicrob. Agents Chemother.*, **36**, 733 (1992).
[41] K.D. Hargrave, J.R. Proudfoot, K.G. Grozinger, E. Cullen, S.R. Kapadia, U.R. Patel, V.U. Fuchs, S.C. Mauldin, J. Vitous. *J. Med. Chem.*, **34**, 2231 (1991).
[42] A.S. Kashina, G.C. Rogers, J.M. Scholey. *Biochim. Biophys. Acta*, **1357**, 257 (1997).
[43] Z. Maliga, T.M. Kapoor, T. Mitchison. *J. Chem. Biol.*, **9**, 989 (2002).
[44] J.C. Cochran, S.P. Gilbert. *Biochemistry*, **44**, 16633 (2005); (b) J.C. Cochran, T.C. Krzysiak, S.P. Gilbert. *Biochemistry*, **45**, 12334 (2006).
[45] A. Goulet, W.M. Behnke-Parks, C.V. Sindelar, J. Major, S.S. Rosenfeld, C. Moores. *J. Biol. Chem.*, **287**, 44654 (2012).
[46] M.-G. Mendoza-Ferri, C.G. Hartinger, R.E. Eichinger, N. Stolyarova, K. Severin, M.A. Jakupec, A.A. Nazarov, B.K. Keppler. *Organometallics*, **27**, 2405 (2008).
[47] R.D. Henkel, J.L. van deBerg, R.A. Walsh. *Anal. Biochem.*, **168**, 312 (1988).